PHARMACEUTICAL BIOLOGY
2022, VOL. 60, NO. 1, 1137–1147
https://doi.org/10.1080/13880209.2022.2079678

Taylor & Francis
Taylor & Francis Group

RESEARCH ARTICLE

OPEN ACCESS Check for updates

Camel milk protein hydrosylate alleviates hepatic steatosis and hypertension in high fructose-fed rats

Mohammad A. Alshuniaber[a], Ghedeir M. Alshammari[a], Samy M. Eleawa[b], Abu ElGasim A. Yagoub[a], Abdullrahman S. Al-Khalifah[a], Maha H. Alhussain[a], Laila Naif Al-Harbi[a] and Mohammed Abdo Yahya[a]

[a]Department of Food Science and Nutrition, College of Food and Agricultural Sciences, King Saud University, Riyadh, Saudi Arabia; [b]College of Health Sciences, Applied Medical Sciences Department, PAAET, Safat, Kuwait

ABSTRACT

Context: Camel milk is used in traditional medicine to treat diabetes mellitus hypertension and other metabolic disorders.

Objective: This study evaluated the antisteatotic and antihypertensive effects of camel milk protein hydrolysate (CMH) in high fructose (HF)-fed rats and compared it with the effects afforded by the intact camel milk protein extract (ICM).

Materials and methods: Adult male Wistar rats were divided into 6 groups ($n = 8$ each) as 1) control, 2) ICM (1000 mg/kg), 3) CMH (1000 mg/kg), 4) HF (15% in drinking water), 5) HF (15%) + ICM (1000 mg/kg), and 6) HF (15%) + CMH (1000 mg/kg). All treatments were given orally for 21 weeks, daily.

Results: Both ICM and CMH reduced fasting glucose and insulin levels, serum and hepatic levels of cholesterol and triglycerides, and serum levels of ALT and AST, angiotensin II, ACE, endothelin-1, and uric acid in HF-fed rats. In addition, both ICM and CMH reduced hepatic fat deposition in the hepatocytes and reduced hepatocyte damage. This was associated with an increase in the hepatic activity of AMPK, higher PPARα mRNA, reduced expression of fructokinase C, SREBP1, SREBP2, fatty acid synthase, and HMG-CoA-reductase. Both treatments lowered systolic and diastolic blood pressure. However, the effects of CMH on all these parameters were greater as compared to ICM.

Discussion and conclusions: The findings of this study encourage the use of CMH in a large-scale population and clinical studies to treat metabolic steatosis and hypertension.

ARTICLE HISTORY
Received 13 July 2021
Revised 19 April 2022
Accepted 14 May 2022

KEYWORDS
Metabolic disorder; hyperlipidaemia; hyperglycaemia; liver; angiotensin; NAFLD; blood pressure

Introduction

The microbial or digestive hydrolysis of protein is a new strategy that leads to the production of several new bioactive compounds with many health-beneficial effects. Currently, it is largely accepted that the addition of such bioactive peptides or protein hydrolysates to our diet may protect against several disorders due to their antioxidant, antihypertensive, antidiabetic, and anticarcinogenic properties (Kilara and Panyam 2003). Indeed, studies have generated several antioxidant bioactive compounds from the hydrolysis of several proteins from sunflower, bovine milk, camel milk, soybean protein, and egg white (Megías et al. 2004; Cinq-Mars et al. 2008; Al-Shamsi et al. 2018).

Camel milk is a basic nutritional source for many people living in the Arabian arid areas. It is believed to have many health-beneficial effects that protect against many chronic disorders (Alhaj 2020). Camel milk is popular in the Africa and Arabian Gulf region, especially in Saudi Arabia, and is consumed daily as fresh and soured milk (Kumar et al. 2016a; Alhaj 2020). Our previous studies have shown that fermented camel milk has potent antihypertensive effects in spontaneously induced hypertensive rats (SHR) due to its high content of bioactive peptides generated by the active bacterial (Yahya et al. 2017). After enzymatic hydrolysis, camel milk protein hydodrosylate (CMH) showed potent and stronger antioxidant effects as compared to bovine milk hydodrosylate (BMH) (Salami et al. 2011; Kumar et al. 2016b; Al-Shamsi et al. 2018). Also, a total of 12 angiotensin-converting enzyme inhibitory peptides were identified from the water-soluble permeates of fermented camel milk using *Lactobacillus helveticus* and *Lactobacillus acidophilus* (Alhaj 2020).

Fructose is consumed in high amounts in Western diets, and it is used as a sweetener in the food industry. During the last decades, the consumption of high fructose (HF) has dramatically increased and was associated with the development of chronic disorders such as obesity, diabetes mellitus (DM), insulin resistance (IR), hypotension, and metabolic syndromes (Bray et al. 2004). Indeed, short and long-term administration of HF diet leads to the rapid development of hypertension and metabolic syndrome (Rizkalla 2010; Mondal et al. 2019). Of interest, in a very recent study, Kilari et al. (2021) showed that CMH has potent hypoglycaemic, antihyperlipidemic, and antioxidant potential in diabetic rats.

However, the effects of CMH on HF-diet-induced metabolic syndrome and hypertension were poorly investigated. Therefore, this study hypothesised that short-term administration of CMH will attenuate hyperglycaemia, IR, hypertension, and hyperlipidaemia in a rat model of HF-induced hypertension and metabolic

CONTACT Ghedeir M. Alshammari aghedeir@ksu.edu.sa Department of Food Science and Nutrition, College of Food and Agricultural Sciences, King Saud University, Riyadh, 11451, P.O. Box 2460, Saudi Arabia

syndrome. Also, we have investigated if the hypotensive effect of CMH is mediated by an ACEI-inhibitory activity.

Materials and methods

Regular and CMH preparation

The preparation of the CMH was performed following previous studies with some modifications (Wang et al. 2020). Fresh camel milk was purchased from a private farm in Riyadh, KSA. We have analysed this camel milk in our laboratory and found the following contents: 3.3% fat, 4% protein, 4.2% lactose, and pH = 6.23. The camel's milk was first defatted, and lactose was removed by incubating with lactase (0.5 g/L) for 3 h at 37 °C. The rate of lactose hydrolysis was determined to be 83%, and the remaining lactose fraction was less than 7%. This lactose-free milk was then divided, as described below, into either regular or hydrolysate casein fractions (namely intact milk and CMH, respectively) and converted to powder via freeze-drying. For preparing CHM, the lactose-free camel milk was placed in HCl solution (pH = 3) and incubated with pepsin enzyme at a 200:1 (w/w) ratio for 2 h at 37 °C. The pepsin activity was stopped by increasing the pH to 8. Trypsin was then added to the mixture (200:1) (w/w) and incubated for 2 h at 50 °C. The trypsin reaction was stopped by heating for 15 min at 80 °C. The degree of hydrolysis was determined as described by Kumar et al. (2016a) and was found to be more than 85%. In this study, the proteolytic enzymes including pepsin and trypsin were added to improve the ACE-inhibitory activity of camel milk, as previously reported by Salami et al. (2010). Hydrolysate samples were converted to powder via freeze-drying and kept in the freezer until the day of use.

Animals

Adult male Wistar rats weighing 150–200 g were obtained from the Animal house unit at the College of Pharmacy, King Saud University (KSU), Riyadh, KSA. In this study, we considered male rats due to the key role of androgens in the development of fructose-induced hypertension (Song et al. 2004). Rats were housed individually (1 rat/cage), under controlled conditions (25 °C, 12 h light/dark cycle, and 50 ± 5% relative humidity). During the experimental procedure, all rats had free access to the normal diet (AIN-93M, Cat. No. D10012Mi, Research Diets, USA) (3.81 Kcal/9% fat, 76% carbohydrates, and 15% proteins) (Table 1) and drinking water. All protocols used in this study followed the guidelines provided by the ethical research committee at KSU (ethical number 108-EACC-2015).

Experimental design

Rats were randomly divided into 6 groups ($n = 8$/group) as 1) control rats: received drinking water as a vehicle; 2) ICM-treated rats: were control rats and received ICM extract at a final dose of 1000 mg/kg; 3) CMH-treated rats: were control rats and received CMH at a final concentration of 1000 mg/kg; 4) HF-fed rats: Fed high fructose HF solution (15%, v/v) dissolved in the drinking water; 5) HF + ICM-treated rats: received concomitant HF-solution (15%) and ICM extract (1000 mg/kg body weight; and 6) HF + CMH-treated rats: received concomitant HF solution (15%) and CMH (1000 mg/kg body weight. All treatments were administered daily for 21 weeks. Administration of the vehicle, ICM, and CMH was given orally using a gavage needle.

Table 1. Composition of the AIN-39M control diet.

Classic description	Ingredients	Normal diet g/diet
Protein	Cystine, L	1.8
Protein	Casein, Lactic, 30 Mesh	140
Carbohydrate	Starch.corn	495.69
Carbohydrate	Lodex 10	125
Carbohydrate	Sucrose	100
Fiber	Solka Floc, FCC200	40
Fat	Soybean Oil, USP	40
Minerals	S10022M	35
Vitamins	V10037	10
Vitamin	Choline bitartrate	2
Antioxidant	*tert*-Butylhydroquinone (tBHQ)	0.01
Total		**1000**
Carbohydrates		76%
Protein		15%
Fat		9%
Total calorie (kcal/g)		**3.81**

Rats were housed individually, and water and food intake were monitored daily. The HF regimen was adopted from the study of Mašek et al. (2020), which has shown that daily treatment with 15% HF in water for 20 weeks can induce hepatic steatosis and hypertension. The single tested dose of CMH (1000 mg/kg) was chosen based on our dose-response preliminary data, which examined the hypolipidemic effect of increasing doses ranging from 100–1000 mg/kg. The dose of 1000 mg/kg showed the maximum hypolipidemic effect in this part.

Body weights and blood pressure measurements

Rat body weights were measured at day 0 (beginning of the experiment) and then every week for 21 weeks. Systolic blood pressure (SBP), diastolic blood pressure (DBP), and heart rate value (HR) were measured by the end of the study using the tail-cuff non-invasive method using the CODA 20830 instrument, Kent Scientific Corporation, Torrington, CT, USA). The animals were adapted for the pressure machine for 5 repeated measurements/day during the experimental period.

Serum and tissue collection

By the end of week 21, rats were fasted for 12 h and then anaesthetised with a mixture of 80/12 mg/kg ketamine/xylazine solution (i.m.) (cat K-113 Sigma Aldrich, St. Louis, MO, USA). Blood samples were withdrawn by the cardiac puncture procedure into plain tubes, centrifuged at 1200 *g* for 10 min, and the supernatants were isolated and stored at −80 °C for further analyses. The livers were removed from all rats of all groups, snap-frozen in liquid nitrogen, and stored at −80 °C for further analysis.

Extraction of hepatic lipids

Lipid extraction from the liver samples was conducted as previously reported by Folch et al. (1957). In brief, 0.5 g tissue of the frozen liver of each rat was homogenised using a Potter-Elvehjem homogeniser 10 mL methanol: chloroform solution (1:2 v/v) (in ice). The homogenate of each sample was filtrated using a filter paper to recover the liquid phase, which was shaken in Buchler Evapo-Mix for 1 h at 4 °C. The 2 mL normal saline was added. The whole mixture was vortexed for 30 sec and then centrifuged at 1400 *g* at 4 °C for 10 min. The lower organic chloroform layer was isolated to new tubes and evaporated in a rotary

evaporator under a vacuum. The isolated lipids were dissolved in 500 µL isopropanol. All samples were stored at −20 °C and used later for the analysis of various lipids.

Biochemical analysis of glucose and insulin levels in the serum

Serum levels of glucose and insulin were measured in all samples ($n = 8$) using a special rat assay and ELISA kits (Cat. No. 10009582 Cayman Chemical, MI, USA, and Cat. No. 589501, Ann Arbour, MI, USA). The homeostasis model assessment of insulin resistance (HOMA-IR index) was calculated as demonstrated by Roza et al. (2016) using the following equation: HOMA-IRI = ([fasting glucose concentration (mg/dL) × fasting insulin concentration (ng/mL)]/405).

Biochemical analysis in the serum

Serum levels of alanine aminotransferase (ALT), aspartate aminotransferase (AST), and gamma-glutamyl transpeptidase 1 (γ-GGT) were measured by ELISA kits (Cat. No. CSB-E13024r, Cat. No. CSB-E13023r, and Cat. No. CSB-EL009394RA, CUSABIO, TX. USA respectively). The total CHOL and LDL-c levels were measured using a rat specific assay kit (Cat No. 80106, BIOLABS, France and Cat. No. 79960, Crystal Chem, IL, USA). Total levels of TGs were measured by a colorimetric kit (Cat. No. 10010303, Cayman, MI, USA). Serum levels of uric acid were measured by an assay kit (Cat. No. MBS7606443, MyBioSource, TX, USA). Serum levels of angiotensin I converting enzymes (ACE), ANG II, and endothelin-1 were measured using rat specific ELISA kit (Cat. No. MBS2516052, Cat. No. MBS705139, and Cat. No. MBS263783, MyBioSource, TX, USA, respectively). All analyses were performed for $n = 8$ samples/group and per each kit's instructions.

Liver homogenates and measurements of oxidative stress-related parameters

Parts of the frozen liver samples (40 mg) were homogenised in 0.5 mL phosphate-buffered saline (PBS) (pH = 7.4) and then centrifuged at 4 °C for 15 min at 112,000 *g*. The collected supernatants were stored at −80 °C and used later to measure the oxidative stress-related parameters. Hepatic levels of malondialdehyde (MDA), superoxide dismutase (SOD), and total reduced glutathione (GSH) were measured using rat specific ELISA kits (Cat. No. MBS268427, Cat. No. MBS036924, and Cat. No. MBS265966, respectively). Hepatic levels of reactive oxygen species (ROS) were measured using a fluorometric kit (Cat. NO. STA-347; Cell Biolabs, CA, USA).

Real-time polymerase chain reaction

Real-time PCR was conducted to measure the mRNA levels of the sterol regulatory element-binding proteins (SREBP 1 and 2), the peroxisome proliferator-activated receptor alpha (PPARα), fatty acid synthase (FAS), HMG-CoA reductase (HMGCoAR), and β-actin. All primers used in this reaction are shown in Table 2. In brief, the total RNA was isolated using the miRVana kit (Cat. No. A27828, ThermoFisher Scientific) and reversed transcribed using the Verit thermal cycler in a 96-well plate using the following ingredients: 10 µL Ssofast Evergreen Supermix, 2 µL cDNA (500 ng/µL), 0.4 µL of 10 µM forward primer (200 nm/reaction), 0.4 µL of 10 µM reverse primers (200 nm/reaction), and 7.2 µL of nuclease-free water. qPCR reaction steps were 1) enzyme inactivation (95 °C, 1 cycle, 30 sec) and 2) denaturation (95 °C, 5 sec) and annealing (60 °C, 60 sec) for 40 cycles, and 3) melting and a final melting step (1 cycle, 95 °C, 30 sec). Levels of mRNA of each gene were quantified by the associated software using the ΔΔCT method and β-actin as a reference. All procedures were conducted according to the manufacturer's instructions for 6 samples/groups.

Western blotting

Parts of frozen livers (70 mg) were homogenised in a radioimmunoprecipitation (RIPA) buffer (Cat ab156034, Abcam Cambridge, UK) in the presence of a protease and phosphatase inhibitor cocktail. The homogenates were centrifuged for 15 min at 1100 *g* at 4 °C, and supernatants containing the protein fractions were collected and transferred to new tubes protein levels on all samples were measured by a protein assay kit (Ab156034, Cambridge, UK). Samples were prepared in the loading dye at a final protein concentration of 2 µg/µL and boiled for 5 min in a water path. Equal protein concentrations were separated on 12% SDS-PAGE, transferred on nitrocellulose membrane, blocked with 5% skimmed milk, and washed 3 times with 1X Tris-buffered Saline-Tween 20 (TBST) buffer. The membranes were then incubated overnight with the primary antibodies (prepared in TBST buffer) at 4 °C against AMPK (Cat. No. sc-130394, 1:1000, 63 kDa), p-AMPK (Thr172) (Cat. No. sc-33524, 500, 63 kDa), ketohexokinase (fructokinase C) (Cat. No. sc-377411, 1:1000, 33 kDa, and β-actin (Cat. No. 47778, 1:10000, 45 kDa). The membranes were then rewashed with the TBST buffer and incubated with the horseradish peroxidase (HRP)-conjugated secondary antibody (prepared in TBST buffer). Then, the bands were

Table 2. Primers are used in the quantitative real-time PCR reaction (qPCR).

Gene	Primers	GenBank accession #	Annealing temperature	Product length
SREBP-1c	F:5′-GCA AGG CCA TCG ACT ACA TC-3′ R:5′-TTT CAT GCC CTC CAT AGA CAC-3′	NM_001276707.1	60 °C	161
SREBP-2	F:5′-CTGACCACAATGCCGGTAAT-3′ R:5′-CTTGTGCATCTTGGCATCTG-3′	NM_001033694.1	60 °C	204
PPAR-α	F:5′-TGCGGACTACCAGTACTTAGGG-3′ R:5′-GCTGGAGAGAGGGTGTCTGT-3′	NM_013196.1	60 °C	116
FAS	F:5′-GCC ATT TCC ATT GCC CTTAGC-3′ R:5′-CTG AGC CAA GCA CCG CACACT-3′	NM_017332	60 °C	273
HMGCoAR	F:5′-TGTTCAAGGGGCGTGCAAAGACAA-3′ R:5′-TCAAGCTGCCTTCTTGGTGCATGT-3′	NM_013134	60 °C	202
β-actin	F:5′-ATC TGG CAC CAC ACC TTC-3′ R:5′-AGC CAG GTC CAG ACG CA-3′	NM_031144	60 °C	291

developed using an ECL pierce kit (Cat 32109, ThermoFisher), scanned, and photographed using the C-Di Git blot scanned and associated software (LI-COR, USA). An internal standard sample was run on all different gels and used for normalisation. The expression of all target genes was expressed relative to the expression of β-actin by dividing the intensity of each band of interest over the intensity of the corresponding band of the β-actin. The average values for the expression of each protein were expressed as mean ± SD of all analysed samples.

Histopathological examination

Livers were collected in 10% buffered formalin solution for 24 h. All liver sections were dehydrated in ascending concentrations of alcohol (70–100%). After that, the tissues were then cleared with xylene and embedded in paraffin. Using a microtome, all sections were cut at 3-5 µm sections and processed for staining with haematoxylin and eosin (H&E). All sections were examined by a pathologist who was unaware of any of the experimental groups. All images were captured under a light microscope (Model Nikon eclipse E200, Japan).

Statistical analysis

GraphPad Prism statistical software (V8, Australia) was used for statistical analyses. Normality was tested using the Shapiro-Wilk test. All analyses were conducted using a two-way analysis of variance (ANOVA) followed by Tukey's *post hoc* test. The values were presented as mean ± standard deviation (SD) and were considered significantly different ta $p < 0.05$.

Results

Changes in the levels of fasting glucose, fasting insulin, and lipid profiles

Administration of the ICM and CMH to control rats didn't affect final body weights and liver weights as compared to control rats (Table 3). However, lower levels of fasting blood glucose and insulin, serum and hepatic levels of TGs and CHOL, serum levels of LDL-c, and values of HOMA-IR were seen in ICM and CMH-treated rats as compared to control rats (Table 3). As compared with other groups, HF-fed rats showed a significant increase in body and liver weights as well as in the levels of all biochemical constituents of serum and hepatic lipid levels, which were significantly reduced in HF + ICM and HF + CMH-treated rats (Table 3). The levels of all these parameters were significantly higher in HF + CMH as compared to HF + ICM-treated rats (Table 3).

Effects on hepatic fat deposition and liver structure

Normal histological structures, including intact rounded hepatocytes radiating from a central vein and normally appearing sinusoids, were observed in the livers of the control, ICM, and CMH-treated rats (Figure 1A–C). However, increased fat droplet accumulation of all sizes with abnormally dilated central veins was observed in the HF-fed rats (Figure 1D). A significant reduction in fat droplet accumulation with almost normal hepatic structures was observed in the livers of both the HF + ICM and HF + CMH-treated rats (Figure 1E & F). Despite these improvements, some fatty changes and accumulation of cytoplasmic fat were observed only in the livers of HF + ICM-treated rats but not in the livers of HF + CMH-treated rats (Figure 1E).

Effects on hepatic markers of oxidative stress

Levels of ROS and MDA were significantly increased in the livers of HF-fed rats as compared to control rats (Figure 2A–D). Administration of ICM and CMH to control rats or HF-fed rats significantly lowered levels of ROS and MDA and stimulated the levels of GSH and SOD as compared to either control or HF-fed rats (Figure 2A–D). In both treated groups, the reduction in ROS and MDA and the increase in the SOD and GSH were significantly more profound in the groups treated with CMH than those that received ICM (Figure 2A–D). Also, no significant variations in the levels of ROS, MDA, GSH, and SOD were observed when HF + CMH-treated rats were compared with the control rats (Figure 2A–D).

Effects on the serum levels of liver injury markers and the hepatic expression of fructokinase C

ICM and CMH-treated rats showed normal ALT and AST levels as compared to control rats (Figure 3A & B). However, serum levels of uric acid and hepatic protein levels of fructokinase C have significantly reduced in the ICM and CMH-treated rats as compared to control rats (Figure 3A–D). On the other hand, serum levels of ALT, AST, and uric acid, as well as the protein

Table 3. Final body and liver weight as well as serum and hepatic lipid levels in all groups of rats.

	Control	Control + IMC	Control + CMH	HF-diet	HF + IMC	HF + CMH
Food intake (g/rats/week)	187 ± 13.2	176 ± 17.1	181 ± 14.9	129 ± 13.1^{abc}	119 ± 11.9^{abc}	123 ± 14.8^{abc}
Water consumption (ml/day)	34.2 ± 7.1	33.4 ± 6.4	35.1 ± 8.9	48.4 ± 6.8^{abc}	44.3 ± 5.9^{abc}	49.1 ± 7.6^{abc}
Final body weight (g)	446 ± 22.8	435 ± 28.1	439 ± 19.8	589 ± 32^{abc}	501 ± 21.5^{abcd}	429 ± 21.2^{de}
Serum						
Liver weight	15.2 ± 1.2	14.7 ± 1.4	15.5 ± 1.1	22.6 ± 1.3^{abc}	18.2 ± 1.1^{abcd}	14.4 ± 1.4^{de}
TGs (mg/dl)	41.2 ± 4.6	35.8 ± 4.2^{a}	28.1 ± 3.7^{ab}	74.3 ± 6.3^{abc}	53.4 ± 6.2^{abcd}	44.5 ± 4.9^{bcde}
CHOL (mg/dl)	73.2 ± 6.4	64.3 ± 5.3^{a}	56.9 ± 4.3^{ab}	112 ± 8.7^{abc}	89.7 ± 7.6^{abcd}	75.6 ± 7.1^{bcde}
LDL-c (mg/dl)	28.7 ± 3.5	23.4 ± 3.1^{a}	18.6 ± 1.9^{ab}	61.3 ± 4.8^{abc}	54.1 ± 5.7^{abcd}	30.2 ± 4.4^{bcd}
Glucose (mg/dl)	106.2 ± 5.7	97.8 ± 5.8^{a}	91.5 ± 4.4^{ab}	186 ± 12^{abc}	152.3 ± 8.3^{abcd}	112. 5 ± 7.3^{de}
Insulin (ng/ml)	4.8 ± 0.43	4.01 ± 0.47^{a}	3.65 ± 0.58^{ab}	8.9 ± 1.2^{abc}	6.4 ± 0.92^{abcd}	4.3 ± 0.81^{de}
HOMA-IR	1.13 ± 0.21	0.75 ± 0.15^{a}	0.62 ± 0.19^{ab}	3.3 ± 0.38^{abc}	1.9 ± 0.23^{abcd}	0.99 ± 0.22^{cde}
Hepatic						
TGs (µg/g)	688 ± 68	592 ± 58^{a}	522 ± 51^{ab}	1402 ± 89^{abc}	1022 ± 91^{abcd}	732 ± 88^{bcd}
CHOL (µg/g)	219 ± 15.3	187 ± 11.5^{a}	163 ± 13.2^{ab}	598 ± 22^{abc}	419 ± 19.5^{abcd}	229 ± 21.8^{abd}

Data are presented as mean ± SD for $n = 8$ rats/group. Values are considered significantly different at $p < 0.05$. [a]: significantly different as compared to control rats, [b]: significantly different as compared to control + intact camel milk (ICM)-treated rats. [c]: significantly different as compared to control + camel milk hydrosylate (CMH)-treated rats. [d]: significantly different as compared to high fructose (HF)-fed rats, and [e]: significantly different as compared to HF + ICM-treated ra.

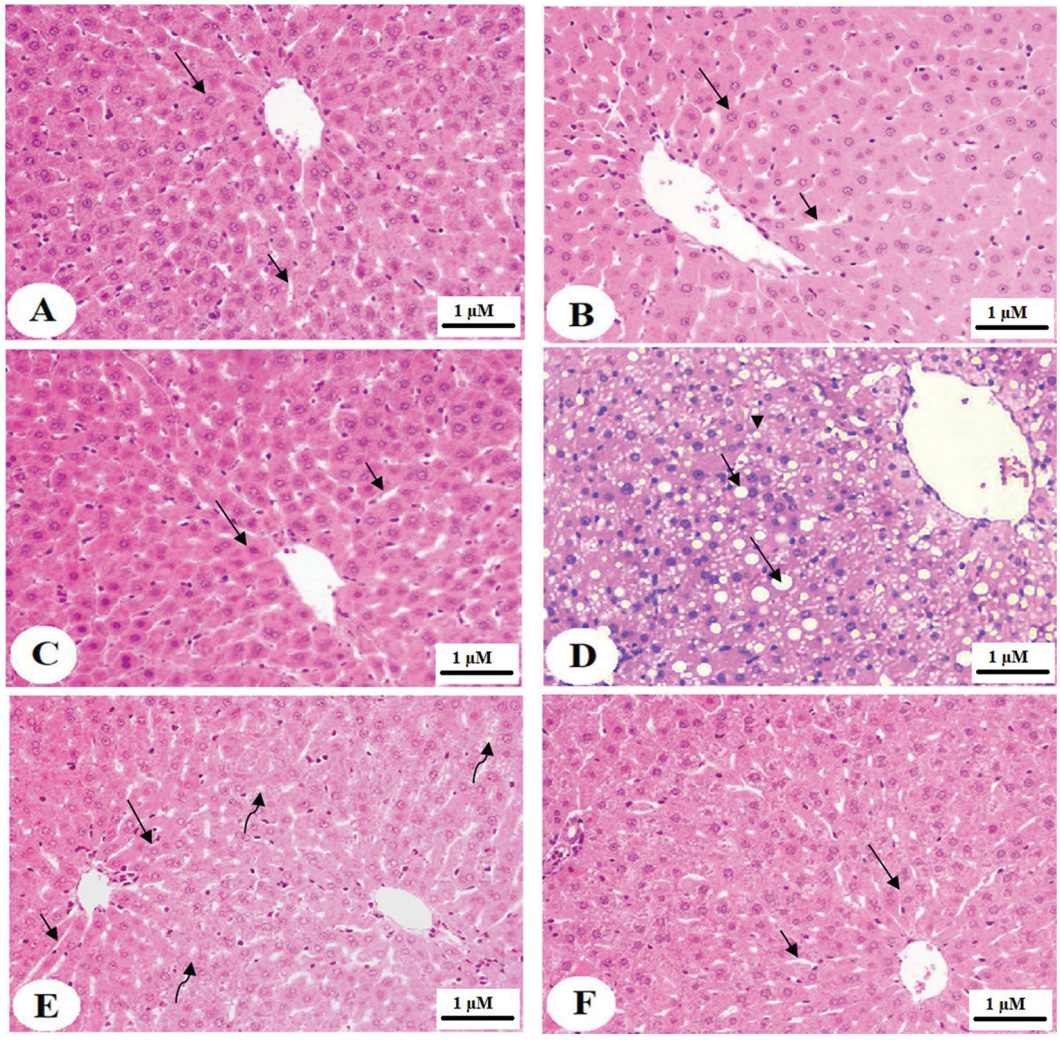

Figure 1. Histological sections of the livers of all groups of rats as stained by the haematoxylin and eosin (H&E). (A–C) were taken from control, intact camel milk (ICM), and camel milk hydrosylate (CMH)-treated rats, respectively, and showing normal liver structure with intact rounded hepatocytes (long arrow) radiating from the central vein (CV) and normally appeared sinusoids (short arrow). (D) was taken from high fructose (HF)-fed rat and showed increased fat droplet deposition of all sizes, including large (long arrow), medium (short arrow), and small vacuoles (arrowhead). The sinusoids were hardly seen. (E) was taken from HF + ICM-treated rats and showed much improvement in the structure of the hepatocytes with an obvious reduction in the fatty vacuolation and normally appeared hepatocytes (long arrow) and sinusoids (short arrow). However, some cytoplasmic lipid accumulation is still seen in some hepatocytes (curved arrow). (F) was taken from HF + CMH and showed almost normal hepatic architecture with no fat accumulation and normal hepatocytes (long arrow) and sinusoids (short arrow) structures.

levels of fructokinase C were significantly increased in the HF-fed rats as compared either to the control and the other groups of rats (Figure 3A–D). Nonetheless, serum levels of all these markers, as well as the hepatic expression of fructokinase C, were significantly decreased in both HF + ICM and HF + CMH, as compared to HF-fed rats (Figure 3A–D). However, the serum levels of uric and the hepatic protein levels of fructokinase C were significantly lower in CMH-treated rats and HFD + CMH as compared to either ICM-treated rats or HF + ICM-treated rats, respectively (Figure 3C & D). No significant variation in serum levels of ALT, AST, and uric acid was seen when HF + CMH-treated rats were compared with the control rats (Figure 3A–D). However, hepatic levels of fructokinase C in the HF-CMH-treated rats remained significantly lower than those in the control rats (Figure 3D).

Effects on serum levels of ET-1, ANG II, and ACE

Serum levels of ANGII, ACE, and ET-1, as well SBP and DBP, were significantly increased in HF-fed rats as compared to control rats (Figure 4A–D). Although ICM-treated rats showed a significant reduction in the serum levels of ANG II, ACE, and ET-1, as well as in the levels of both SBP and DBP as compared to control rats, there were no significant variations in the levels of all these parameters between HF-fed rats and HF + ICM-treated rats (Figure 4A–D). On the contrary, there was a significant reduction in the serum levels of ANG II, ACE, and ET-1, as well as in the levels of both SBP and DBP in HF + CMH-treated rats as compared to either the control or HF-fed rats (Figure 4A–D). However, the reduction in the levels of all these parameters was more profound in CMH-treated rats as compared to ICM-treated rats (Figure 4A–D). Interestingly, serum levels of ANGII, ACE, and ET-1, as well as in SBP and DBP measured in HF + CMH-treated rats were not significantly different from their corresponding levels depicted in the control rats (Figure 4A–D).

Changes in the hepatic expression of AMPK, PPARα, and SREBP1/2

Total hepatic levels of AMPK were not significantly varied among all measured groups of rats (Figure 5A). As compared

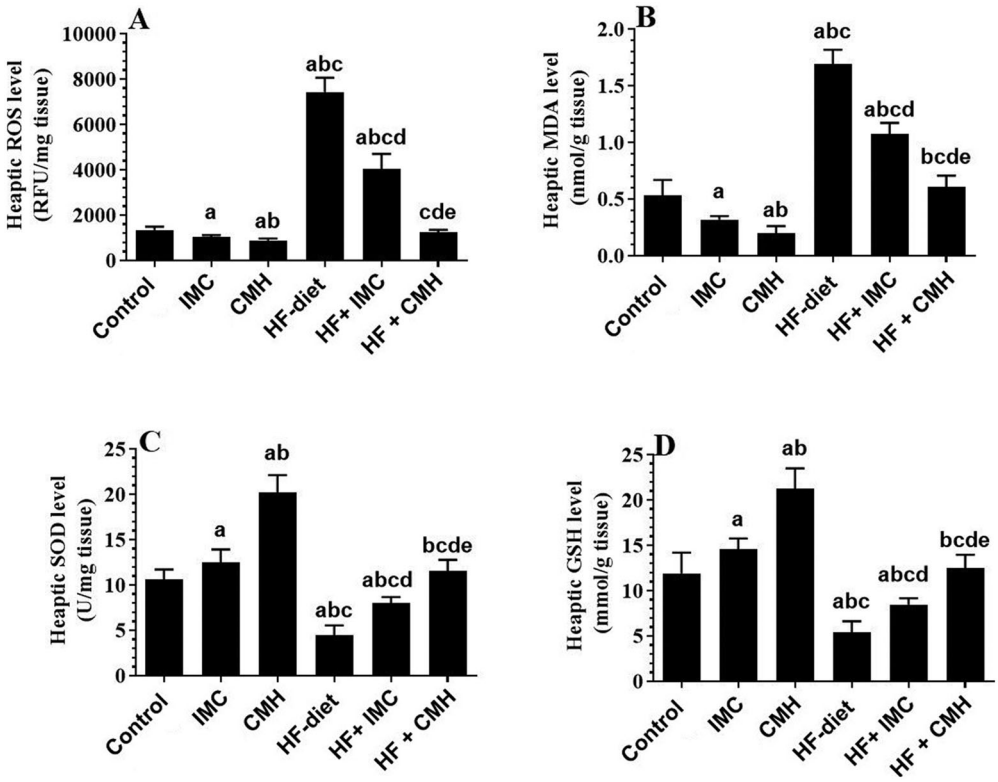

Figure 2. Hepatic levels of ROS (A), MDA (B), SOD (C), and GSH (D) in all groups of rats. Data are presented as mean ± SD for $n = 8$ rats/group. Values are considered significantly different at $p < 0.05$. [a]: significantly different as compared to control rats, [b]: significantly different as compared to intact camel milk (ICM)-treated rats. [c]: significantly different as compared to camel milk hydrosylate (CMH)-treated rats. [d]: significantly different as compared to high fructose (HF)-fed rats, and [e]: significantly different as compared to HF + ICM-treated rats.

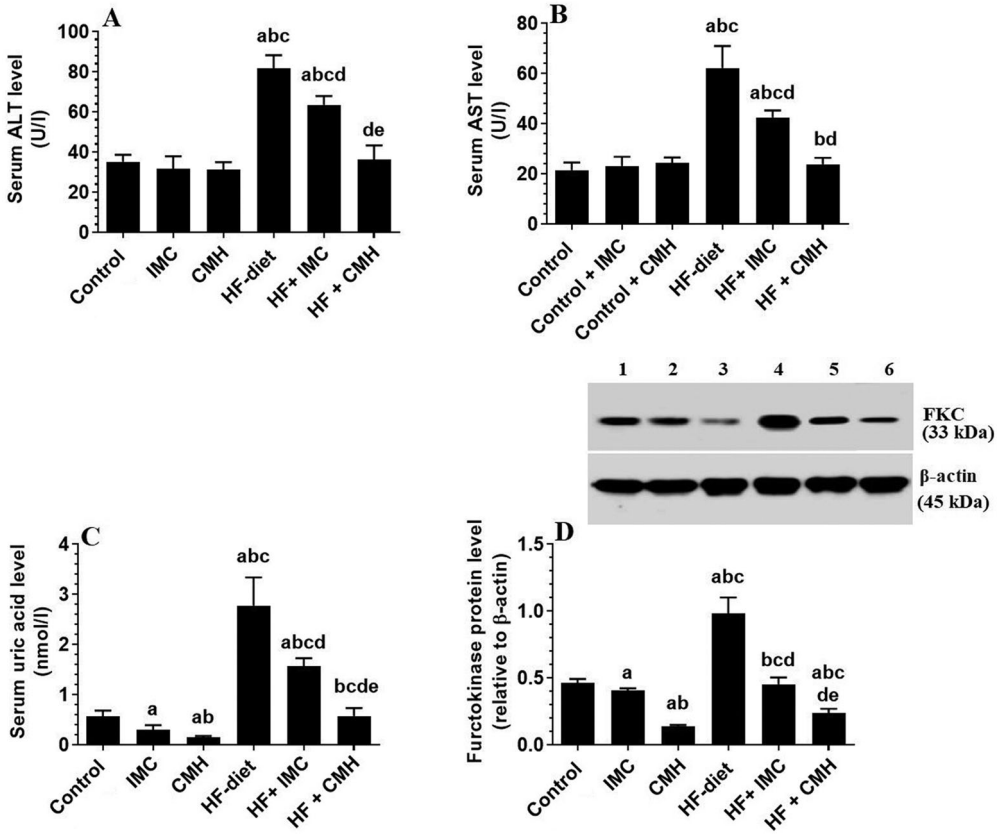

Figure 3. Serum levels of ALT (A), AST (B), and uric acid (C), as well hepatic protein levels of fructokinase C (D) in all groups of rats. Data are presented as mean ± SD for $n = 8$ rats/group. Values are considered significantly different at $p < 0.05$. Values are considered significantly different at $p < 0.05$. [a]: significantly different as compared to control rats, [b]: significantly different as compared to intact camel milk (ICM)-treated rats. [c]: significantly different as compared to camel milk hydrosylate (CMH)-treated rats. [d]: significantly different as compared to high fructose (HF)-fed rats, and [e]: significantly different as compared to HF + ICM-treated rats.

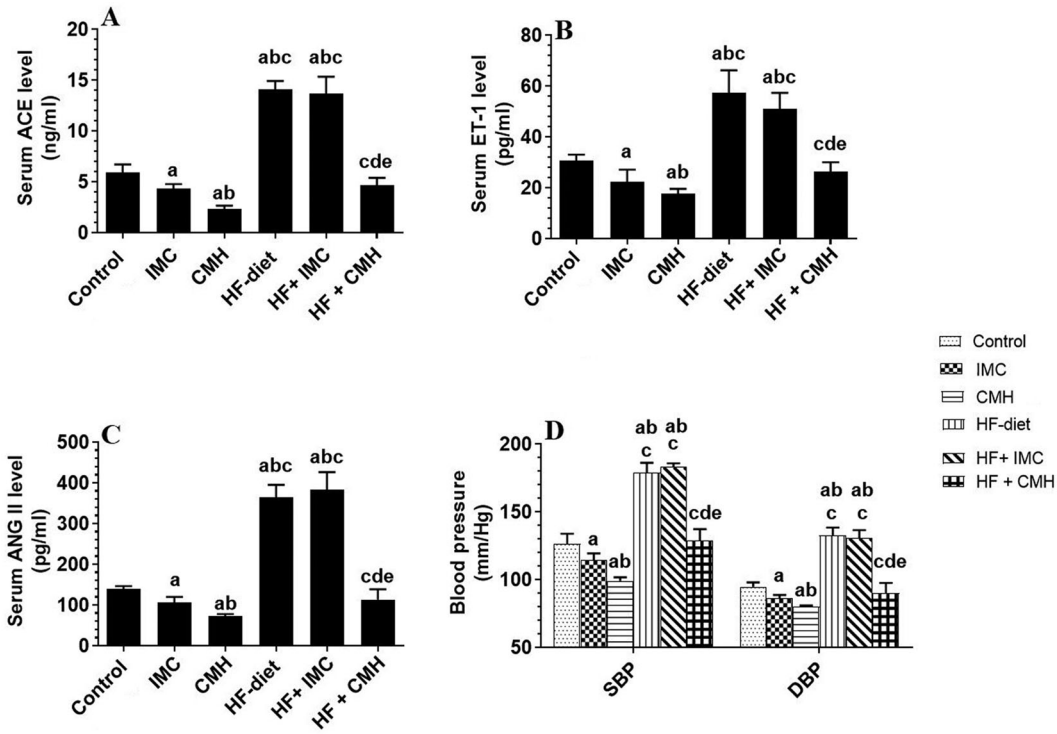

Figure 4. Serum levels of ACE (A), ET-1 (B), and ANG II (C), as well as the systolic and diastolic blood pressures (SBP/DBP) (D) in all groups of rats. Data are presented as mean ± SD for $n = 8$ rats/group. Values are considered significantly different at $p < 0.05$. Values are considered significantly different at $p < 0.05$. [a]: significantly different as compared to control rats, [b]: significantly different as compared to intact camel milk (ICM)-treated rats. [c]: significantly different as compared to camel milk hydrosylate (CMH)-treated rats. [d]: significantly different as compared to high fructose (HF)-fed rats, and [e]: significantly different as compared to HF + ICM-treated rats.

with control rats, HF-fed rats had a significant decrease in the ratio of p-AMPK/AMPK, and mRNA levels of PPARα accompanied by a significant increase in mRNA levels of SREBP 1, SREBP 2, FAS, and HMGCoAR (Figure 5A–D). On the other hand, protein levels of p-AMPK (Thr172), a ratio of p-AMPK/AMPK, and mRNA levels of PPARα were significantly increased, and mRNA levels of SREBP1, SREBP2, FAS, and HMGCoAR were significantly decreased in the livers of both the control or HF-fed rats which were administered either ICM or CMH as compared to control or HG-fed rats (Figure 5A–D). Of note, the increase in the hepatic protein levels and the ratio of p-AMPK and levels of PPARα, as well as the reduction in the hepatic mRNA levels of SREBP1, SREBP2, FAS, and HMGCoAR, were more profound in CMH-treated rats and HF + CMH-treated rats as compared to either the ICM-treated rats or HF + ICM-treated rats, respectively (Figure 5A–C). There were no significant variations in the levels of all these markers between HF + CMH-treated rats and control rats (Figure 5A–C).

Discussion

The salient findings of this study showed that short-term administration of CMH attenuates HF-rich diet-induced hyperglycaemia, hyperlipidaemia, IR, and hepatic steatosis in rats, an effect that is greater than that afforded by ICM. According, several mechanisms of protection are reported, including 1) hypoglycaemic and insulin-sensitizing effects, 2) suppressing the hepatic fructokinase C and the subsequent production of uric acid, 3) upregulating hepatic antioxidants, and 4) activating AMPK and subsequent downregulation of the sterol regulatory element-binding proteins 1 and 2 (SREBP1/2 and upregulation of the transcription factor the peroxisome proliferator-activated receptor α (PPARα), and 5) inhibiting ANG II synthesis and ACE activation. To the best of our knowledge, these data are the first to mechanistically explain such protective effects afforded by CMH in metabolically impaired animals. A summary of these effects is shown in the graphical abstract (Figure 6).

In this study, the chronic consumption of an HF-rich diet was associated with increased final body weights, adiposity, and increased HF solution uptake but with a significant reduction in food intake, attributed to appetite suppression. However, an HF-rich diet can regulate the appetite by modulating the expression of the peripheral (e.g., ghrelin and leptin) and central hypothalamic appetite peptide [e.g., peptide YY (PYY), neuropeptide Y (NPY), and proopiomelanocortin (POMC)] (Lowette et al. 2015). Currently, this effect is still contradictory and seems to be dependent on the dose and treatment period (Lowette et al. 2015). Indeed, and similar to our data, chronic consumption of 15% and 20% HF solution for 60, 70, and 90 days in rodents significantly increased body weights, lipogenesis, and adipogenesis but reduced food intake (Jürgens et al. 2005; Ramos et al. 2017). On the contrary, administration of a 23% HF diet for 2 weeks stimulated food intake and body weight (Lindqvist et al. 2008). On the other hand, the observation that both ICM and CMH were able to attenuate all measured parameters without altering the HF consumption or food intake in both the control and HF-fed rats dissipates the role of these mechanisms in the protection afforded by these diets and indicates that alternative direct mechanisms mediate theses anti-metabolic and antisteatotic effects. Supporting our data, administration of camel milk to diabetic patients didn't affect their appetite, food intake, or serum levels of appetite hormones, including ghrelin, PYY, glucagon-like peptide 1 (GLP-1), and pancreatic polypeptide (PP) (Zheng et al. 2021).

The reduction in serum levels of fasting glucose and insulin levels, as well as values of HOMA-IR in both the control and

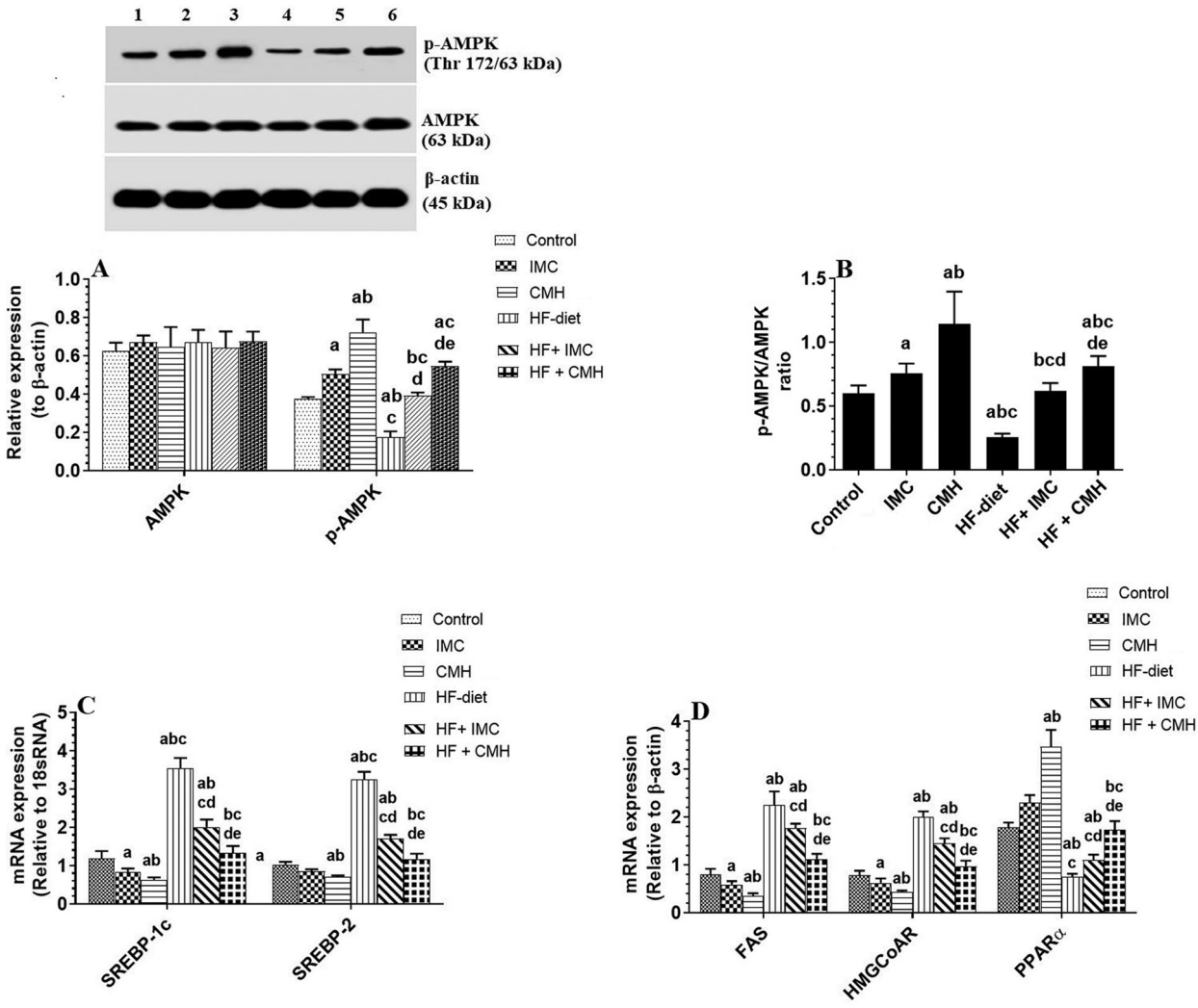

Figure 5. Protein levels of AMPK/p-AMPK (A) and mRNA levels of SREBP1, SREBP2 (B), PPARα, FAS, and HMGCoAR (C) in all groups of rats. Data are presented as mean ± SD for $n = 8$ rats/group. Values are considered significantly different at $p < 0.05$. Values are considered significantly different at $p < 0.05$. [a]: significantly different as compared to control rats, [b]: significantly different as compared to intact camel milk (ICM)-treated rats. [c]: significantly different as compared to camel milk hydrosylate (CMH)-treated rats. [d]: significantly different as compared to high fructose (HF)-fed rats, and [e]: significantly different as compared to HF + ICM-treated rats.

HF-fed rats after treatment with ICM and CMH, suggest potent hypoglycaemic and hypolipidemic effects of both diets. However, the impact of CMH on these markers was more profound than those exerted by ICM. These data are in the same line as those of Kilari et al. (2021), who demonstrated that CMH could attenuate fasting hyperglycaemia in diabetic rats. In the same line, several other investigators have shown that ICM, fermented camel milk, and CMH have potent hypoglycaemic effects in diabetic patients and animals (Kilari et al. 2021; Zheng et al. 2021). However, the hypoglycaemic potential of camel milk has been largely discussed and attributed to several ingredients, including the high content of insulin, insulin-like amino acids and peptides, immunoglobulins (the camelids; IGg1-3), antioxidant vitamins (e.g., vitamins C and E), and immunomodulators which can reduce stimulate insulin secretion, improves insulin sensitivity, and reduce fasting glucose levels by suppressing oxidative stress, preventing the damage of pancreatic beta cells, and enhance glucose uptake and utilisation (Ayoub et al. 2018; Zheng et al. 2021). However, our data indicate that both ICM and CMH reduce HF-induced insulin levels. These results suggest that both treatments do not affect insulin release but rather improve its sensitivity, which accounts for the observed hypoglycaemic effect.

In this study, we have also shown the potential of CMH to suppress serum and hepatic lipid levels in both the control and HF-fed rats to a greater extent rather than in the ICM. These data also support many other previous studies that demonstrated camel milk's ability to reduce serum levels of TGs, CHOL, and LDL-c in diabetic individuals and other animal models (Al-Numair 2010; Ejtahed et al. 2014; Zheng et al. 2021). In this view, the hypolipidemic effect of camel milk was attributed to the previously discussed insulin and insulin-like amino acids, which could suppress the activity of the lipoprotein lipase (Al-Numair 2010). In addition, camel milk can inhibit CHOL synthesis and transport by activating the enzyme lecithin cholesterol acyltransferase enzyme (LCAT), inhibiting the 3-hydroxy-3-methylglutaryl-CoA (HMG-CoA) reductase, and modulating the activity of the thyroid hormone through unknown mechanisms and ingredients (Ibrahim et al. 2017; Zuberu et al. 2017). Also, the hypolipidemic effect of camel milk was attributed to its antioxidant potential and the high content of vitamins C and E (Badr et al. 2017; Zuberu et al. 2017).

Associated with these effects, we have also shown that both ICM and CMH have potent antioxidant effects not only in the livers of HF-fed rats but also in the livers of control rats through depleting ROS and upregulating SOD and GSH. Generally, ROS

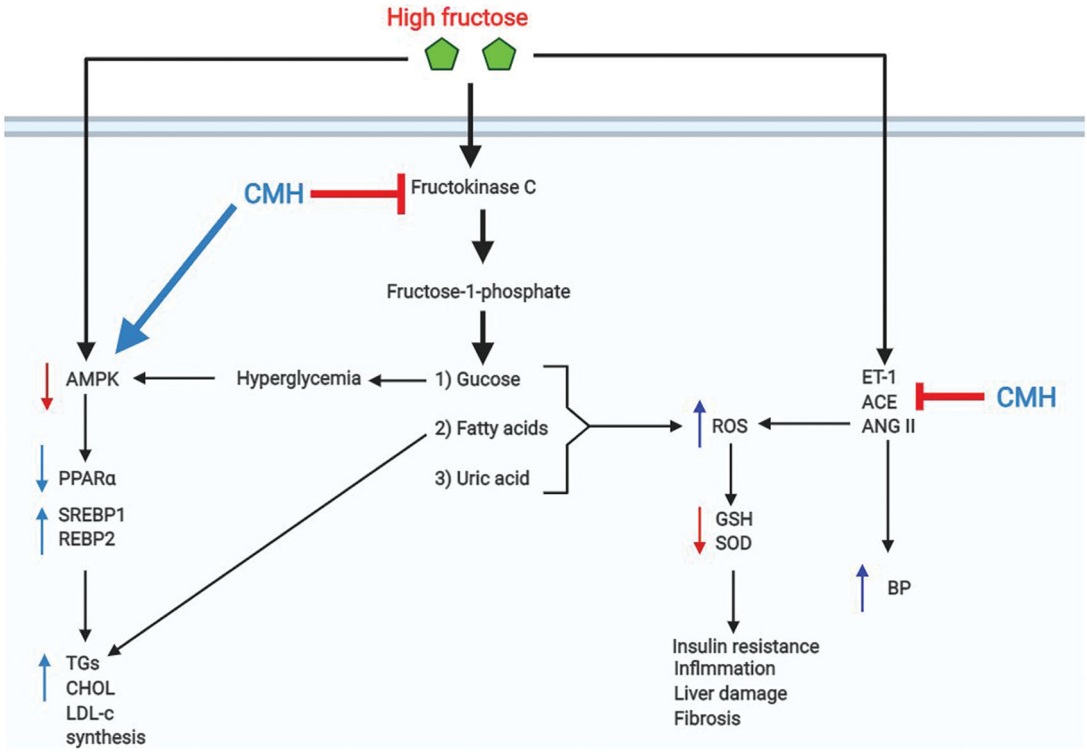

Figure 6. A graphical abstract demonstrating the protective effect of the camel milk hydrosylate (CMH) against high fructose diet-induced hypertension, hyperglycaemia, and non-alcoholic fatty liver disease (NAFLD). All steps are assumed to occur in the liver tissue. The mechanisms include 1) downregulating the hepatic fructokinase C enzyme, which results in suppressing the production of glucose, fatty acids, and uric acid; 2) upregulating antioxidants; 3) activating AMPK and PPARα, which inhibits lipogenesis by suppressing SREBP1/2 and activating and fatty acids oxidation, respectively; and 4) inhibiting the production of ANG II possibly by downregulating endothelin-1 (ET-1) and angiotensin-converting enzyme (ACE). TGs: triglycerides; CHOL: cholesterol, ROS: reactive oxygen species; CPT1/2: carnitine palmitoyltransferase I/2.

is a major hallmark of HF-induced hepatic steatosis by promoting inflammation, IR, and steatosis (Vos and Lavine 2013; Jegatheesan and De Bandt 2017; Chen et al. 2020). Given the stimulatory effect of both ICM and CMH on GSH and SOD in the livers of the control and HF-fed rats, we can strongly argue that such antioxidant potential is mediated by a direct upstream mechanism such as activation of the nuclear factor erythroid 2–related factor 2 (Nrf2), a master antioxidant transcription factor (Ma 2013). This effect could also be attributed to their high vitamins C and E content, directly scavenging ROS. Supporting our data, evidence from *in vivo* and *in vitro* studies has also shown potent ROS scavenging abilities of enzymatically hydrolysed camel milk CMH (Kumar et al. 2016a; Al-Shamsi et al. 2018). A similar observation was reported by many authors where the antioxidant potential of CMH was stronger than that produced by the enzymatic hydrolysis of bovine casein (Salami et al. 2011; Kumar et al. 2016a).

Despite the extensive research in diabetic and HFD-fed animals, the precise molecular mechanisms underlying the antidiabetic and antisteatotic effect of ICM and CMH in HF-fed animals is largely unknown. Recent studies have shown that CMH can lower blood glucose levels by decreasing carbohydrate digestion and inhibiting glucose production by suppressing the α-amylase, dipeptidyl peptidase-IV (DDP-4), and α-glucosidase, effects that were more effective than the intact milk (Mudgil et al. 2018; Nongonierma et al. 2019). However, the major damaging mechanism by which HF-rich diet-induced liver damage, oxidative stress, steatosis, and fibrosis was reported to be due to the activation of the key limiting hepatic enzyme, named fructokinase C (FKC), which catalyses the conversion of fructose to fructose-1-phosphate (F1P) (Vos and Lavine 2013; Jegatheesan and De Bandt 2017; Zuberu et al. 2017). Once hyperactivated, this substrate is sustainedly converted to glucose, fatty acids, lactate, and uric acid to promote hyperglycaemia, hyperlipidaemia, oxidative stress, lipogenesis, and IR (Tappy & Lê 2010; Jegatheesan and De Bandt 2017). Nevertheless, uric acid is a very toxic molecule that stimulates the generation of massive quantities of ROS and induces hepatic oxidative damage, inflammation, IR, and fibrosis by scavenging antioxidants, depletion of ATP, activation of NADPH oxidase, upregulation of the transforming growth factor-β1, and inducing mitochondria damage and endoplasmic reticulum (ER) stress (Vos and Lavine 2013; Jegatheesan and De Bandt 2017). Indeed, knocking down FKC is an effective therapeutic strategy to alleviate HF-diet-induced hyperlipidaemia, IR, and hepatic steatohepatitis (Ishimoto et al. 2013).

In this study, the observations that ICM and CMH reduce the serum levels of uric acid and the hepatic expression of FKC in both the control and HF-fed rats is clear evidence that the antihyperglycemic, antihyperlipidemic, and antioxidative effects of these diets are mediate, at least, by suppressing this enzyme. Therefore, our data suggest that both ICM and CMH are negative upstream regulators of this enzyme's activity. However, the precise mechanism by which CHM exerts this is still not determined and needs further investigation. Yet, we still can't exclude the above-discussed mechanisms of camel milk from such protective effects.

AMPK is a conserved energy molecule that stimulates catabolic pathways to produce ATP by suppressing lipogenesis, glucose uptake, and utilisation and stimulating FAs oxidation (Li et al. 2011; Wang et al. 2018). As a key molecule, AMPK suppresses TGs and CHOL synthesis by downregulating the transcription factors SREBP1, and SREBP2, respectively (Li et al.

2011). On the other hand, AMPK stimulates FAs oxidation by activating the transcription factor PPARα, which stimulates the carnitine system (CPT1 and CPT2) (Yoon 2009). Also, AMPK stimulates the peripheral uptake of glucose and improves insulin sensitivity by increasing glucose receptors (GLUT4) expression (Chopra et al. 2012). Of note, hyperglycaemia and AMPK are negatively crossed with each other, where higher fasting glucose levels inhibit hepatic and muscular AMPK activation, but AMPK suppresses hepatic gluconeogenesis and stimulates peripheral glucose uptake and glycogen synthesis (Jeon 2016; Lin and Hardie 2018; Agius et al. 2020).

Levels of AMPK and PPARα are significantly depleted, whereas levels of SREBP1/2 are significantly increased in HF-fed animals and were shown to be major mechanisms for the associated hepatic steatosis (Jegatheesan et al. 2015; Herman and Samuel 2016; Jegatheesan and De Bandt 2017; Woods et al. 2017). This has also been seen in HF-fed rats in this study. However, pharmacological activation of AMPK prevented HF-induced hepatic steatosis in rodents (Woods et al. 2017). In this study, our novelist finding is that both ICM and CMH significantly stimulated the activation of AMPK in the livers of both the control and HF-fed rats, which could explain the concomitant increase in the levels of PPARα and the decrease in the levels of SREBP1/2 and their target genes (FAS and HMGCoAR). Until now, we are still unsure whether its activation is a direct effect secondary to the observed hypoglycaemic impact of these diets. The relation seems bidirectional, and further studies using transgenic animals are needed to confirm this relationship.

Nevertheless, hypertension is the major clinical manifestation associated with HFD (Klein and Kiat 2015). HF-rich diet-induced hypertension is an independent mechanism that is not related to HF-induced NAFLD and IR (Klein and Kiat 2015). Studies have shown that an HF-rich diet induces hypertension by several interconnected mechanisms, including increasing sodium and chloride absorption, as well as upregulation and increased release of ET1, which subsequently induces activation of ANG II, stimulates the synthesis of TXA2, and reduces levels of nitric oxide (NO) in the (reviewed in Klein and Kiat 2015). ACE inhibitors effectively reduced the elevated SBP and DBP in HF-fed rats, thus suggesting that the activation of ANG II is the most effective mechanism in HF-induced hypertension (Erlich and Rosenthal 1995; Kim et al. 2020). Previous studies using bosentan, a dual ET-1 receptor antagonist, prevented HF-induced ANG II and hypertension, suggesting that the increases in ANG II are due to HF-induced activation of ET-1 receptors (Tran et al. 2009). In this study, both ICM and CMH significantly reduced both the SBP and DBP and reduced circulatory levels of ANG II, ACE, and ET-1 in both the control and HF-fed rats. Again, these effects were more profound in rats fed the CMH. These data suggest that ICM and CMH lower BP by attenuating the ET-1/ANG II axis, as well as suppressing ACE. However, since ANG II is a potent inducer of ROS through the direct activation of NADPH oxidase (Hitomi et al. 2007), these data may implicate that the antioxidant potentials of the CMH could also be mediated by suppression of ANG II. Although this study is unique for HF-fed rats, we and others have previously shown the hypotensive effect of camel milk and skimmed fermented camel milk in high salt-induced hypertensive rats (Mainasara et al. 2016; Yahya et al. 2017).

Despite these data and extensive available literature, our study still has some limitations. Most importantly, we are still unable to precisely identify the active ingredients in the CMH which are responsible for all these effects. In addition, we also can't explain why the inhibitory effect of CMH on this enzyme was greater than that of milk. In addition, our findings are still observational and need a more advanced experiment to confirm these mechanisms and draw a potential link between them. Also, since the products of CMH produced *in vitro* by enzymes could be close to products that can be produced *in vivo*, this may produce peptides with similar biological activity that we can't determine in this study. Therefore, further studies to compare the effects of the *in vivo* and *in vitro* produced ingredients are required to validate this.

Conclusions

Our study showed a potent potential of CMH to alleviate hepatic steatosis as compared to ICM. This opens a window to use CMH to alleviate hepatic damage and hyperlipidaemia in other animal models, as well as in human subjects with NAFLD. However, this requires further investigations.

Author contributions

Conceptualisation: MAA and ASA: Methodology: GMA and AEAY; Biochemical analysis: MHA, LNA, and MAY; Data curation: GMA and SME; Original Draft Writing & Editing: all authors.

Disclosure statement

The authors declare no conflicts of interest associated with this work.

Funding

The authors extend their appreciation to the Deanship of Scientific Research at King Saud University for funding this work through research group No: RG-1441-435.

ORCID

Ghedeir M. Alshammari http://orcid.org/0000-0002-2043-1209
Laila Naif Al-Harbi http://orcid.org/0000-0003-0778-922X
Mohammed Abdo Yahya http://orcid.org/0000-0002-5665-9600

References

Agius L, Ford BE, Chachra SS. 2020. The metformin mechanism on gluconeogenesis and AMPK activation: the metabolite perspective. IJMS. 21(9): 1137.

Alhaj OA. 2020. Exploring potential therapeutic properties of camel milk. In O. Alhaj, B. Faye, and R. Agrawal (Eds.), Handbook of research on health and environmental benefits of camel products. Hershey (PA): IGI Global. p. 123–154.

Al-Numair KS. 2010. Type II diabetic rats and the hypolipidemic effect of camel milk. J Food Agric Environ. 8:77–81.

Al-Shamsi KA, Mudgil P, Hassan HM, Maqsood S. 2018. Camel milk protein hydrolysates with improved technofunctional properties and enhanced antioxidant potential in *in vitro* and in food model systems. J Dairy Sci. 101(1):47–60.

Ayoub MA, Palakkott AR, Ashraf A, Iratni R. 2018. The molecular basis of the anti-diabetic properties of camel milk. Diabetes Res Clin Pract. 146: 305–312.

Badr G, Ramadan NK, Sayed LH, Badr BM, Omar HM, Selamoglu Z. 2017. Why whey? Camel whey protein as a new dietary approach to the management of free radicals and for the treatment of different health disorders. Iran J Basic Med Sci. 20:338–349.

Bray GA, Nielsen SJ, Popkin BM. 2004. Consumption of high-fructose corn syrup in beverages may play a role in the epidemic of obesity. Am J Clin Nutr. 79(4):537–543.

Chen Z, Tian R, She Z, Cai J, Li H. 2020. Role of oxidative stress in the pathogenesis of nonalcoholic fatty liver disease. Free Radic Biol Med. 152: 116–141.

Chopra I, Li HF, Wang H, Webster KA. 2012. Phosphorylation of the insulin receptor by AMP-activated protein kinase (AMPK) promotes ligand-independent activation of the insulin signalling pathway in rodent muscle. Diabetologia. 55(3):783–794.

Cinq-Mars CD, Hu C, Kitts DD, Li-Chan EC. 2008. Investigations into inhibitor type and mode, simulated gastrointestinal digestion, and cell transport of the angiotensin I-converting enzyme-inhibitory peptides in pacific hake (*Merluccius productus*) fillet hydrolysate. J Agric Food Chem. 56(2):410–419.

Ejtahed HS, Niasari Naslaji A, Mirmiran P, Zraif Yeganeh M, Hedayati M, Azizi F, Moosavi Movahedi A. 2014. Effect of camel milk on blood sugar and lipid profile of patients with type 2 diabetes: a pilot clinical trial. Int J Endocrinol Metab. 13(1):e21160.

Erlich Y, Rosenthal T. 1995. Effect of angiotensin-converting enzyme inhibitors on fructose induced hypertension and hyperinsulinaemia in rats. Clin Exp Pharmacol Physiol Suppl. 22(1):S347–S9.

Folch J, Lees M, Sloane Stanley GH. 1957. A simple method for the isolation and purification of total lipides from animal tissues. J Biol Chem. 226(1): 497–509.

Herman MA, Samuel VT. 2016. The sweet path to metabolic demise: fructose and lipid synthesis. Trends Endocrinol Metab. 27(10):719–730.

Hitomi H, Kiyomoto H, Nishiyama A. 2007. Angiotensin II and oxidative stress. Curr Opin Cardiol. 22(4):311–315.

Ibrahim MA, Wani FA, Rahiman S. 2017. Hepatoprotective effect of olive oil and camel milk on acetaminophen-induced liver toxicity in mice. Int J Med Sci Public Health. 6(1):186–194.

Ishimoto T, Lanaspa MA, Rivard CJ, Roncal-Jimenez CA, Orlicky DJ, Cicerchi C, McMahan RH, Abdelmalek MF, Rosen HR, Jackman MR, et al. 2013. High-fat and high-sucrose (western) diet induces steatohepatitis that is dependent on fructokinase. Hepatology. 58(5):1632–1643.

Jegatheesan P, Beutheu S, Ventura G, Nubret E, Sarfati G, Bergheim I, De Bandt JP. 2015. Citrulline and nonessential amino acids prevent fructose-induced nonalcoholic fatty liver disease in rats. J Nutr. 145(10):2273–2279.

Jegatheesan P, De Bandt JP. 2017. Fructose and NAFLD: the multifaceted aspects of fructose metabolism. Nutrients. 9(3):230.

Jeon SM. 2016. Regulation and function of AMPK in physiology and diseases. Exp Mol Med. 48(7):e245.

Jürgens H, Haass W, Castañeda TR, Schürmann A, Koebnick C, Dombrowski F, Otto B, Nawrocki AR, Scherer PE, Spranger J, et al. 2005. Consuming fructose-sweetened beverages increases body adiposity in mice. Obes Res. 13(7):1146–1156.

Kilara A, Panyam D. 2003. Peptides from milk proteins and their properties. Crit Rev Food Sci Nutr. 43(6):607–633.

Kilari BP, Mudgil P, Azimullah S, Bansal N, Ojha S, Maqsood S. 2021. Effect of camel milk protein hydrolysates against hyperglycemia, hyperlipidemia, and associated oxidative stress in streptozotocin (STZ)-induced diabetic rats. J Dairy Sci. 104(2):1304–1317.

Kim M, Do GY, Kim I. 2020. Activation of the renin-angiotensin system in high fructose-induced metabolic syndrome. Korean J Physiol Pharmacol. 24(4):319–328.

Klein AV, Kiat H. 2015. The mechanisms underlying fructose-induced hypertension: a review. J Hypertens. 33(5):912–920.

Kumar D, Chatli M, Singh R, Mehta N, Kumar P. 2016a. Enzymatic hydrolysis of camel milk casein and its antioxidant properties. Dairy Sci & Technol. 96(3):391–404.

Kumar D, Verma A, Chatli M, Singh R, Kumar P, Mehta P, Malav O. 2016b. Camel milk: alternative milk for human consumption and its health benefits. Nutr Food Sci. 46(2):217–227.

Li Y, Xu S, Mihaylova MM, Zheng B, Hou X, Jiang B, Park O, Luo Z, Lefai E, Shyy JY, et al. 2011. AMPK phosphorylates and inhibits SREBP activity to attenuate hepatic steatosis and atherosclerosis in diet-induced insulin-resistant mice. Cell Metab. 13(4):376–388.

Lin SC, Hardie DG. 2018. AMPK: sensing glucose as well as cellular energy status. Cell Metab. 27(2):299–313.

Lindqvist A, Baelemans A, Erlanson-Albertsson C. 2008. Effects of sucrose, glucose and fructose on peripheral and central appetite signals. Regul Pept. 150(1–3):26–32.

Lowette K, Roosen L, Tack J, Vanden Berghe P. 2015. Effects of high-fructose diets on central appetite signaling and cognitive function. Front Nutr. 4(2):5.

Ma Q. 2013. Role of nrf2 in oxidative stress and toxicity. Annu Rev Pharmacol Toxicol. 53:401–426.

Mainasara AS, Isa SA, Dandare A, Ladan MJ, Saidu Y, Rabiu S. 2016. Blood pressure profile and insulin resistance in salt-induced hypertensive rats treated with camel milk A Mediterranean. MNM. 9(1):75–83.

Mašek T, Barišić J, Micek V, Starčević K. 2020. Cafeteria diet and high-fructose rodent models of NAFLD differ in the metabolism of important PUFA and palmitoleic acid without additional influence of sex. Nutrients. 12(11):3339.

Megías C, del Mar Yust M, Pedroche J, Lquari H, Girón-Calle J, Alaiz M, Millán F, Vioque J. 2004. Purification of an ACE inhibitory peptide after hydrolysis of sunflower (*Helianthus annuus* L.) protein isolates. J Agric Food Chem. 52(7):1928–1932.

Mondal K, Gowda KPS, Manandhar S. 2019. Anti-hypertensive effect of *Abelmoschus esculentus* (okra) seed extracts in fructose-induced hypertensive rats. Indian J Physiol Pharmacol. 63:175–181.

Mudgil P, Kamal H, Yuen GC, Maqsood S. 2018. Characterization and identification of novel antidiabetic and anti-obesity peptides from camel milk protein hydrolysates. Food Chem. 259:46–54.

Nongonierma AB, Cadamuro C, Le Gouic A, Mudgil P, Maqsood S, FitzGerald RJ. 2019. Dipeptidyl peptidase IV (DPP-IV) inhibitory properties of a camel whey protein enriched hydrolysate preparation. Food Chem. 279:70–79.

Ramos VW, Batista LO, Albuquerque KT. 2017. Effects of fructose consumption on food intake and biochemical and body parameters in Wistar rats. Rev Port Cardiol. 36(12):937–941.

Rizkalla SW. 2010. Health implications of fructose consumption: a review of recent data. Nutr Metab. 7:82.

Roza NA, Possignolo LF, Palanch AC, Gontijo JA. 2016. Effect of long-term high-fat diet intake on peripheral insulin sensibility, blood pressure, and renal function in female rats. Food Nutr Res. 60(1):28536.

Salami M, Moosavi-Movahedi AA, Ehsani MR, Yousefi R, Haertlé T, Chobert JM, Razavi SH, Henrich R, Balalaie S, Ebadi SA, et al. 2010. Improvement of the antimicrobial and antioxidant activities of camel and bovine whey proteins by limited proteolysis. J Agric Food Chem. 58(6):3297–3302.

Salami M, Moosavi-Movahedi AA, Moosavi-Movahedi F, Ehsani MR, Yousefi R, Farhadi M, Niasari-Naslaji A, Saboury AA, Chobert JM, Haertlé T. 2011. Biological activity of camel milk casein following enzymatic digestion. J Dairy Res. 78(4):471–478.

Song D, Arikawa E, Galipeau D, Battell M, McNeill JH. 2004. Androgens are necessary for the development of fructose-induced hypertension. Hypertension. 43(3):667–672.

Tappy L, Lê KA. 2010. Metabolic effects of fructose and the worldwide increase in obesity. Physiol Rev. 90(1):23–46.

Tran LT, MacLeod KM, McNeill JH. 2009. Endothelin-1 modulates angiotensin II in the development of hypertension in fructose-fed rats. Mol Cell Biochem. 325(1–2):89–97.

Vos MB, Lavine JE. 2013. Dietary fructose in nonalcoholic fatty liver disease. Hepatology. 57(6):2525–2531.

Wang Q, Liu S, Zhai A, Zhang B, Tian G. 2018. AMPK-mediated regulation of lipid metabolism by phosphorylation. Biol Pharm Bull. 41(7):985–993.

Wang R, Han Z, Ji R, Xiao Y, Si R, Guo F, He J, Hai L, Ming L, Yi L. 2020. Antibacterial activity of trypsin-hydrolyzed camel and cow whey and their fractions. Animals (Basel). 10(2):337.

Woods A, Williams JR, Muckett PJ, Mayer FV, Liljevald M, Bohlooly-Y M, Carling D. 2017. Liver-specific activation of AMPK prevents steatosis on a high-fructose diet. Cell Rep. 18(13):3043–3051.

Yahya MA, Alhaj OA, Al-Khalifah AS. 2017. Antihypertensive effect of fermented skim camel (*Camelus dromedarius*) milk on spontaneously hypertensive rats. Nutr Hosp. 34(2):416–421.

Yoon M. 2009. The role of PPARalpha in lipid metabolism and obesity: focusing on the effects of estrogen on PPARalpha actions. Pharmacol Res. 60(3):151–159.

Zheng Y, Wu F, Zhang M, Fang B, Zhao L, Dong L, Zhou X, Ge S. 2021. Hypoglycemic effect of camel milk powder in type 2 diabetic patients: a randomized, double-blind, placebo-controlled trial. Food Sci Nutr. 9(8): 4461–4472.

Zuberu J, Saleh MIA, Alhassan AW, Adamu BY, Aliyu M, Iliya BT. 2017. Hepatoprotective effect of camel milk on poloxamer 407 induced hyperlipidaemic Wistar rats. Open Access Maced J Med Sci. 5(7):852–858.